



Non-linear tide-surge interactions around the coast of the UK through the lens of tidal level, phase, and skew surge

Luke J. Jenkins^{a,*}, Ivan D. Haigh^a, Dafni E. Sifnioti^b, Jose Alejandro Pinto Rascon^b, Addina Inayatillah^a, Hachem Kassem^a

^a School of Ocean and Earth Science, National Oceanography Centre, University of Southampton, European Way, Southampton, SO14 3ZH, UK

^b EDF Research and Development UK Centre, London, W1T 4EZ, UK

ARTICLE INFO

Keywords:

Tide-surge
Interaction
Tidal phase
Skew surge
Residual
Coastal hazards

ABSTRACT

Coastal flooding, driven by extreme sea levels, is a significant threat to the coastline of the United Kingdom. The primary contribution to extreme sea levels is the combination of tide and surge and understanding how these components interact is critical to assessing extreme sea levels at the coast. Here, we analyse the interactions of skew surge and tidal high water, non-tidal residual and tidal phase, and non-tidal residual and tidal level using the entire observational tide gauge network of the UK, a near 500-year model, and a model run of 2013/14 with an artificially adjusted forcing to examine how storm arrival time impacts these interactions. We show that the levels of tide-surge interaction at most sites are relatively insensitive to the magnitude of the extreme value threshold and the declustering window size. Measured data show greater levels of interaction than modelled data and although there is little interaction between skew surge and tidal high water, there are sizeable tide-surge interactions between the non-tidal residual and the astronomical tide, the largest being for tidal phase. Around the UK, extreme non-tidal residuals generally occur favourably between 1 and 5 h before tidal high water and at tidal levels that are at, or below, the average tidal level. When storm arrival time is artificially shifted, the overall change in interaction around the UK is relatively small, with skew surge and non-tidal residual maxima occurring at similar respective tidal high waters, tidal phases, and tidal levels, although variation is seen on smaller spatial scales. Our findings advance the understanding of non-linear tide-surge interactions around the UK, which is essential for the accurate estimation of extreme sea level probabilities and thus the defence of the coastline against coastal flooding.

1. Introduction

Coastal flooding from extreme sea levels is among the costliest and most dangerous natural hazards, with wide ranging social, economic, and environmental impacts. The United Kingdom (UK) has a long history of coastal flood events, the most prominent in the last century being the 'Big Flood' of January 31st to February 1st 1953, where 330 people lost their lives on the east coast of England and Scotland with an estimated £1.2 billion in damages (McRobie et al., 2005). The UK has also seen periods of significant, continued coastal flooding such as in 2013/14, which was the stormiest winter season on record (Matthews et al., 2014). During the December to February period in 2013/14 an intense extra-tropical cyclone hit the UK on average every 2.5 days (Priestley et al., 2017). The high number of storm events and the low inter-event times translated into the highest number of sea level, surge,

and wave threshold exceedance events for a winter season in the UK, also with the highest levels of temporal clustering (Jenkins et al., 2023; Wadey et al., 2015). The UK has seen an annual average of £540 million worth of damages due to coastal flooding (Sayers et al., 2015) presenting a significant risk to coastal assets, such as residential and commercial property, storm surge barriers, and strategic coastal infrastructure, including nuclear power stations. Therefore, flooding is one of the highest priority risks for civil emergencies in the UK (Cabinet Office, 2020).

Coastal flooding from extreme sea levels occurs due to combinations of: a) astronomical tide; b) storm surge; c) waves (particularly wave setup and runoff); and d) relative mean sea level (Pugh and Woodworth, 2014). The stage of the tide is crucial to the creation of extreme sea levels, and in the UK most occur due to moderate skew surges (the absolute difference within a tidal cycle between the maximum measured

* Corresponding author.

E-mail address: L.Jenkins@soton.ac.uk (L.J. Jenkins).

<https://doi.org/10.1016/j.ecss.2025.109323>

Received 31 October 2024; Received in revised form 4 April 2025; Accepted 25 April 2025

Available online 25 April 2025

0272-7714/© 2025 The Authors. Published by Elsevier Ltd. This is an open access article under the CC BY license (<http://creativecommons.org/licenses/by/4.0/>).

sea level and the predicted tidal high water level, irrespective of the time of occurrence: [de Vries et al., 1995](#)) combining with high spring tides rather than simply extreme surges ([Haigh et al., 2016](#)). All four components of extreme sea levels experience topographic amplification near the coast and there are non-linear interactions between the four components ([Haigh et al., 2022](#)). Non-linear interactions between the tidal and storm surge components have been recognised and studied, particularly in the southern North Sea. For example, [Doodson \(1929\)](#) noticed a tendency for surge maxima in the Thames Estuary in the UK to occur most frequently on the rising tide. [Proudman \(1957, 1955\)](#) examined the propagation of an externally forced tide and surge into an estuary of uniform section and highlighted the impact of shallow water and bottom friction on the timing and magnitude of highwater, both for standing and progressing waves. [Rossiter \(1961\)](#) used numerical solutions, again in an idealized estuary, and showed how a negative surge would retard tidal propagation, whereas a positive surge would advance high water, through a combination of depth affecting the wave propagation speed, and depth-dependent frictional terms in the equations of motion. Assessing tide gauge data along the UK east coast, [Prandle and Wolf \(1978a, 1978b\)](#) confirmed the tendency for surge peaks to occur most often on the rising tide. They also used numerical models to conclude that this pattern arises irrespective of the phase relationship between tide and surge in the northern North Sea and separated the contributions to interaction from shallow water and bottom friction. Building on these early studies, [Horsburgh and Wilson \(2007\)](#) analysed sea level data at 5 tide gauges in the North Sea and showed that the mode of peak non-tidal residual occurrence is 3–5 h before the nearest high water. They showed that these patterns can be described using a simple mathematical explanation based on a phase shift of the tidal signal combined with the modulation of surge production due to water depth. Since then, many others have highlighted and examined non-linear interactions between the tide and storm surge components in other regions of the world (e.g., [Dinapoli et al., 2021](#); [Hu et al., 2023](#); [Song et al., 2020](#); [Xiao et al., 2021](#); [Yang et al., 2023](#); [Zhang et al., 2010](#)) and, recently, a global analysis was undertaken by [Arns et al. \(2020\)](#) who found that extreme sea level magnitude can be overestimated by up to 30 % if non-linear interactions are not considered.

The [Horsburgh and Wilson \(2007\)](#) study highlighted that the analysis of non-tidal residuals is problematic since there is not always a genuine atmospheric contribution to large residuals ([Williams et al., 2016](#)). This has encouraged the use of skew surges, rather than non-tidal residuals. An illustration of skew surge is shown in [Fig. 1a](#). Based on an analysis of tide gauge records spanning decades from the UK, the United States, the Netherlands, and Ireland, [Williams et al. \(2016\)](#) assessed the relationship between high tides and skew surges and showed that the magnitude of the height of tidal high water exerts no influence on the size of the

most extreme skew surges. These results justified the assumption of independence between tides and skew surges, which is used for the estimation of extreme sea level probabilities in the UK coastal flood boundary conditions approach ([Batstone et al., 2013](#); [Environment Agency, 2018](#)). Previous methodologies for calculating extreme sea level probabilities around the UK coast (e.g., [Dixon and Tawn, 1994](#)) used empirical relationships between tide and non-tidal residual to account for non-linear interactions.

In this paper, we contrast, for the first time to our knowledge, the main methods that have been applied to UK tide gauge data on regional to national spatial scales, building on the approaches applied by [Horsburgh and Wilson \(2007\)](#); [Haigh et al. \(2010\)](#); and [Williams et al. \(2016\)](#). [Horsburgh and Wilson \(2007\)](#) compared the normalised distribution of the frequency of non-tidal residual events against tidal phase at 6 North Sea sites, also modelling the difference in surge production with, and without, the inclusion of the tide. [Haigh et al. \(2010\)](#), building on the approach of [Dixon and Tawn \(1994\)](#), introduced the use of the Chi-squared test statistic for tidal phase at the time of extreme non-tidal residuals to test for tide-surge interactions at 18 English and French tide gauges in the English Channel. They also undertook the analysis of different temporal periods in a record, applying linear regression to Chi-squared test results to evaluate changes to tide-surge interaction through time. [Williams et al. \(2016\)](#), for 77 tide gauges in Northern Europe and the east coast of the U.S.A, applied Kendall's rank-based correlation (τ) for extreme skew surges (top 1 %) and predicted high water, before comparing the probability density functions (pdf) of high waters against the pdf's of high waters at the time of the top 1 % of skew surges. Then, they evaluated seasonal signals of tide-surge interaction by comparing the pdf of high waters at the time of extreme skew surges for different months that are weighted by their storminess. Finally, [Williams et al. \(2016\)](#) modelled the difference in skew surge at 7 sites when four synthetically generated storms arrive at either a spring, or neap tide. Following some of these methods, we analyse tide-surge interactions and compare results around the UK coastline through the lens of: (1) skew surge against high tidal level; (2) non-tidal residual against tidal level; and (3) non-tidal residual against tidal phase (note it is not possible to assess skew surge against tidal phase, as by definition, each skew surge occurs at high water). We test the levels of tide-surge interaction sensitivity seen with varying event-defining thresholds and 'storm windows' for each of these 'parameter pairs', to highlight differences in interaction seen with varying event definition and declustering methods. We start by using measured sea level data at 45 tide gauges around the UK coast. We then repeat this analysis for a state-of-the-art near 500-year model run of tide and surge under pre-industrial climate conditions ([Howard and Williams, 2021](#)) and compare the measured and modelled results. Then, we implement a

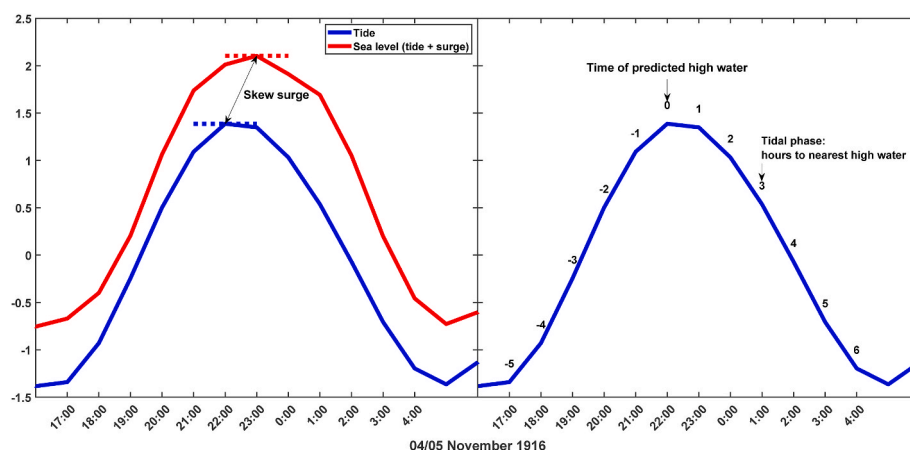


Fig. 1. Illustration of (a) skew surge: the difference between the maximum measured sea level and the predicted tidal high water in a tidal cycle, and (b) tidal phase: the time to the nearest predicted tidal high water.

hydrodynamic modelling exercise to assess the magnitude of non-linear interactions that arise as a result of storms at different times in the tidal cycle, showing how the interactions change with a time-adjusted meteorological forcing and how they alter the extreme sea level magnitude variation.

We have two objectives for our time-series analysis and a third objective for our modelling exercise. For the time-series analysis our objectives are:

1. To examine the sensitivity of tide-surge interactions due to varying event-definition and declustering windows;
2. To determine the levels of tide-surge interaction seen around the UK in the observational record and compare this to the levels seen in a near 500-year model run;

And, for the modelling exercise our objective is:

3. To analyse how tide-surge interaction, and extreme event magnitude, change with shifts in storm arrival time.

2. Data and methods

The analysis was undertaken in two main steps: (1) the time-series analysis, and (2) the hydrodynamic modelling. Each analysis stage is described in the sub-sections below, along with the datasets used.

2.1. Time-series analysis

For this analysis, we utilise measured time-series of tidal level and phase, non-tidal residual, and skew surge to investigate the levels and characteristics of non-linear interactions that occur around the UK. We then repeat this analysis for sea level data from a near 500-year pre-industrial climate model control run and compare the differences in interaction.

2.1.1. Data

The measured data sources used in this stage of analysis are sea level records from the UK National Tide Gauge Network (UKNTGN) that forms part of the Coastal Flood Forecasting Service (UKCFFS). These gauges provide high-frequency measurements of still sea level in hourly frequency before 1993 and 15-min frequency after 1993. Still sea level is the height of the sea surface excluding ocean surface waves, consisting of the astronomical tide, storm surge components and mean sea level variations. Still sea level data records from the gauges were downloaded from the British Oceanographic Data Centre (BODC) website (<http://www.bodc.ac.uk/>).

BODC monitors, retrieves and quality controls the measurements from the tide gauge network. Any flagged values by the BODC quality control were removed and the levels were converted relative to ordnance datum Newlyn (ODN). The 45 tide gauge locations and their regional grouping used in this paper can be seen in Fig. 2.

The modelled data source for the time-series analysis is the dataset of simulated UK storm surges described in Howard and Williams (2021). The authors created the dataset using the National Oceanography

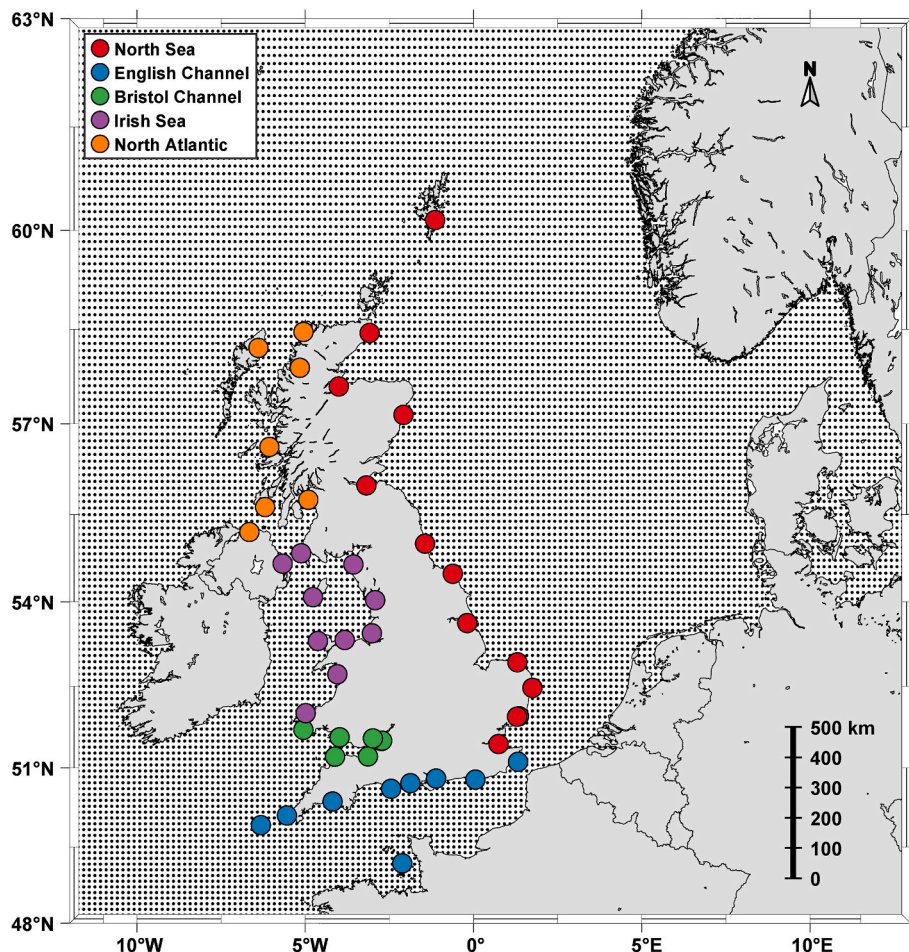


Fig. 2. The Continental Shelf Model 3 model domain and grid nodes, as well as the locations of the UK National Tide Gauge Network tide gauges and their regionalisation used in this study.

Centre's Continental Shelf 3 (CS3) model forced with a 483-year control run of pre-industrial climate from the Hadley Centre Global Environment Model in the Global Couple configuration 3, medium resolution atmosphere, medium resolution ocean numerical model (HadGEM3-GC3-MM) (Williams et al., 2018). CS3 is a depth-averaged barotropic coastal shelf model that has a resolution of $1/9^\circ$ by $1/6^\circ$ (latitude, longitude) and consists of the European shelf region (48N–63N, 12W–13E) (Flather et al., 1991). The 15 largest tidal constituents are applied at the domain lateral boundaries. Typically, when forced with numerical atmospheric data, total water levels produced by CS3 see root mean square errors in the order of 10 cm (Flather, 2000). CS3 was also used for the modelling component of this study. HadGEM3-GC3-MM in the mid-latitudes has a horizontal resolution of $1/4^\circ$ for the ocean and ~ 60 km for the atmosphere. A tide-only run and a tide and surge run were provided, consisting of hourly time-series on a 135 by 150 (latitude by longitude) grid. As the climate conditions were fixed, there is no influence of climate change and mean sea level change was also not included. We determined the grid nodes closest to the measured tide gauges and extracted those time-series for this analysis. The model domain and grid nodes can be seen in Fig. 2.

2.1.2. Data pre-processing

From the measured and modelled data records, we derived 4 time-series, namely: (1) astronomical tide, (2) phase of astronomical tide, (3) non-tidal residual and (4) skew surge.

To calculate astronomical tide levels from the measured sea level records, we first removed relative mean sea level (MSL) trends from the still sea level records to meet the assumption of stationarity in the tidal harmonic analysis. Linear regression was used to estimate MSL trends in a method undertaken by numerous previous sea level studies (Haigh et al., 2009, 2016; Jenkins et al., 2023; Woodworth et al., 2009). This method leaves interannual MSL variability within the time-series by removing annual MSL trends that had been first interpolated to hourly time-series. Harmonic analysis and tidal reconstruction were then undertaken using the MATLAB Unified Tidal Analysis and Prediction Functions (U-Tide) (Codiga, 2022), analysing each calendar year separately. If a year contained less than 50 % of data, the constituents calculated from the harmonic analysis of the nearest year that contained over 50 % of data were used for the tidal reconstruction. Modelled tidal levels were provided within the dataset, so no pre-processing was necessary.

As this research is centred on extreme events and coastal flooding, the timing relative to astronomical high water is of great interest as tides strongly modulate coastal flooding in the UK (Haigh et al., 2016; Jenkins et al., 2023). Therefore 'phase' in this study refers to the time relative to the nearest astronomical high water, as shown in Fig. 1b. To calculate tidal phase, we first identified all the astronomical high waters in the measured and modelled tide time-series. Then we calculated the time to the nearest astronomical high water for every timestep, leaving an equally sized time-series of tidal phase as for the tidal level.

The measured non-tidal residual was calculated simply by subtracting the calculated astronomical tide from the measured still sea level at each tide gauge. Similarly, we subtracted the tide-only modelled time-series from the modelled tide and surge time-series to get the modelled non-tidal residual. The non-tidal residual primarily contains the meteorological contribution termed the 'surge' but may also contain harmonic prediction errors or timing errors and non-linear interactions.

Skew surges, by definition, occur once per tidal cycle. To determine the skew surge values, we used the astronomical high waters identified in the computing of tidal phase and calculated the difference between those and the maximum measured or modelled still sea level for each respective tidal cycle, extracting time-series of skew surges at each tide gauge site or grid node.

2.1.3. Analysis

For the data analysis of the time-series, we combine parts of, and build upon, the different methods of Horsburgh and Wilson (2007), Haigh et al. (2010), and Williams et al. (2016), which to date (to our knowledge) have not been compared and contrasted. We do this for the parameters of: (1) non-tidal residual against tidal level; (2) non-tidal residual against tidal phase; and (3) skew surge against high tidal level.

Initially, we applied Williams et al. (2016) method, testing for the independence of non-tidal residual and skew surge from the tide by analysing whether tidal levels and phases at the time of extreme events have the same statistical distribution as all the respective tidal levels or phases, and whether skew surges have the same distribution as tidal high waters. If the distributions are the same, then one can conclude that the variables are independent from one another. We utilised a Gaussian kernel density estimator (kde) to estimate probability density functions (pdf/s), first to get 100 evaluation points for the population (e.g., 100 tidal phases from all the tidal phases in a time-series), then to use those evaluation points to undertake a kde pdf of the population, and lastly to get a kde pdf of the sample (e.g., tidal phases at time of extreme non-tidal residuals evaluated along the same 100 evaluation points derived from the entire tidal phase time-series). For skew surge and tidal levels, the bandwidth for the kernel smoothing function was calculated through the 'plug-in' method (*aka* improved Sheather-Jones) that utilises an adaptive, Gaussian kernel density estimator based on smoothing properties of the most general linear diffusion process, with an estimated limiting and stationary probability density reducing bias and error. The properties of estimator are used to compute an optimal, non-parametric bandwidth selection (Botev et al., 2010). For tidal phase, as the data is integers with relatively little variation/range (number of hours to nearest tidal high water), the plug-in method smoothed the data too much and Silverman's rule of thumb method (Silverman, 1986) for bandwidth calculation did not smooth the data enough. Instead, a bandwidth of 1 was given as it represented the minimum difference between data points pre-1993 and gave a smoothing that got rid of the inherent 'spikiness' of tidal phase but still illustrated the whole range of values. To enable results at different sites to be directly comparable, each of the pdf distributions (population and sample) at each site were normalised by dividing by the max value of the combined results.

First, to evaluate our first objective we tested the levels of tide-surge interaction seen in the measured and modelled data with varying event-defining thresholds and declustering windows for each parameter, highlighting the difference in interaction seen with varying event and declustering methods. For the threshold selection, we chose the 95th, 97th, and 99th percentiles. We chose the 99th percentile as it represents a magnitude that could constitute a flooding hazard, and the sensitivity testing showed that there were no significant differences with the threshold selection. It also aligns with Williams et al. (2016), who noted that such a threshold stopped the potential error of lower magnitude skew surges resulting from errors within the predicted tidal high waters. The 95th and 97th percentiles were then chosen as lower thresholds, as these were high enough to still be considered as 'extreme', yet low enough in magnitude to potentially highlight differences to the 99th percentile. For the declustering, we followed the 'storm window' approach of Haigh et al. (2016) and Jenkins et al. (2023), where values are sorted by magnitude and then windows of time around each largest value in turn are deleted. Despite both studies using the same method and focusing on the same study region, they used different 'storm window' periods of 84 h (3.5 days) and 32 h (1.33 days), respectively. Therefore, to test tide-surge interaction sensitivity to the declustering window length, we chose to utilise the windows used in those studies plus an additional window of 60 h (2.5 days) that represents a window between the two. We plotted and overlaid the pdfs of the samples for each parameter pair that were calculated at the varying thresholds and declustering windows. This shows the difference in distribution

magnitude and shape (representing interaction) with differing magnitudes and declustering windows.

Next, for our second objective we tested for the independence of non-tidal residual and skew surge from the tide by analysing whether tidal levels and phases at the time of extreme events have the same distribution as all the respective tidal levels or phases, and examined whether skew surges have the same distribution as all high tidal levels. Again, as the sensitivity testing showed that there were no significant differences with the threshold selection and declustering window length, we decided to proceed with the 99th percentile as the threshold to avoid any potential skew surge errors associated with predicted tidal high water errors, and a declustering window of 32 h as it is the smallest window which allows for the inclusion of any quick succession clustering. For both measured and modelled data, at each site, we used the calculated pdfs of the samples and the populations and plotted the difference in the distribution magnitude across the evaluation points. This corresponds to all the parameter pairs: tidal high waters at the time of extreme skew surges and all tidal high waters; tidal phase at the time of extreme non-tidal residuals and all tidal phases; and tidal level at the time of extreme non-tidal residuals and all tidal levels (as mentioned above, we cannot analyse skew surges against tidal phase).

To test if the population and sample distributions for each of the three parameter pairs are statistically different from each other (which would imply that there are significant non-linear interactions between parameters), we applied a Chi-squared goodness of fit test. Haigh et al. (2010) split tidal levels and phases at the time of extreme non-tidal residuals into equiprobable bands and then used the Chi-squared test statistic (χ^2) to test if tidal level and non-tidal residual were independent. If independent, you would expect to see an equal number of non-tidal residuals per tidal level/phase band, so the larger the χ^2 the greater the dependence as the number of extreme non-tidal residuals per band is further from the expected number. We repeated this analysis with a slight adjustment, changing the constant expected number (counts) of extreme-related observations in each equally sized band to instead match the relative proportion of tidal levels/phases seen in the whole time-series for the corresponding band. This better represents the actual distributions of level/phase in varying tidal regimes. However, the large, varying sample sizes from our data may bias the Chi-squared test, particularly across different sites. To address this, we applied Cramer's V (ϕ_c) effect size measurement for the Chi-squared test to negate the effect that the number of observations has on the results. This enabled direct comparison between sites and parameters, with Cramer's V providing a ϕ_c value between 0, indicating no association, and 1, indicating complete association. Thus, in this context, a ϕ_c value of 1 indicates that there is a strong likelihood that the sample distribution, e.g., tidal levels at the time of extreme non-tidal residuals, is completely distinct from the expected distribution that is calculated from the population, e.g., all tidal levels. For the measured and modelled data, at all sites, the χ^2 and then the ϕ_c were calculated for the three parameter pairs.

2.2. Hydrodynamic modelling

In the second stage of this study, we carried out a hydrodynamic modelling exercise to assess the magnitude of non-linear interactions that occur during storms events when the timing of the meteorological forcing, which drives the surge component of sea level, is altered backwards and forwards in time. We do this across all the sites in the UKNTGN, following a similar approach of Haigh et al. (2014) and Williams et al. (2016).

2.2.1. Event selection

We chose to model the years of 2013 and 2014 as this encompassed the entire 2013/14 winter season, which was unprecedented in its number of events and the temporal clustering of those events (Jenkins et al., 2023; Matthews et al., 2014; Priestley et al., 2017).

2.2.2. Model setup and simulations

We used the CS3 depth averaged hydrodynamic model (see Section 2.1.1) to simulate the water levels for each of the storm events. This model was used, until recently, by the Met Office to forecast extreme water levels around the UK. It is considered as one of the world's most extensively validated operational storm surge forecasting models (Flather et al., 1991).

For the years of 2013/14, we downloaded u and v -components of wind velocity (at 10 m) and mean sea level pressure from the ERA5 meteorological re-analysis (Hersbach et al., 2020) covering the area of 12°W to 13°E and 48°N to 63°N (same region as CS3), to encompass the hydrodynamic model domain. These data were used as the meteorological forcing input to the CS3 model to generate surge for the simulation. The temporal resolution of the ERA5 dataset is hourly and the spatial resolution is 0.25° (~35 km), which we interpolated to the ~12 km model resolution of CS3.

A simulation was run for tide-only, and then another simulation was run with tide where the hydrodynamic model was driven by the meteorological forcing from ERA5. Then, we ran another 4 additional simulations in which the hydrodynamic model's meteorological forcing was artificially adjusted by -6, -3, +3 and +6 h. Most of the storm events' peak non-tidal residuals coincided approximately with high water, hence, the -6 shift corresponds with the previous low water, -3 shift with peak flood, +3 with peak ebb, and +6 with the following low water. For these simulations, we converted the meteorological forcing from ERA5 to CS3 format and shifted the meteorological data forward and backward. The results for each model grid cell were saved on an hourly frequency. We extracted the time-series from each simulation run and simply subtracted the tide-only simulation from the tide and surge simulations to gain the non-tidal residual. We then calculated the tidal phase and skew surge in the same manner as we did for the time-series for stage 1 of the analysis.

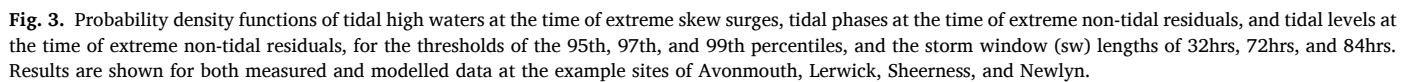
2.2.3. Analysis

The same approach as in stage 1 (time-series data analysis), bar the varying threshold and storm window analysis, was used to analyse the results of every time-shifted simulation to assess the interactions that arise due to storms occurring at different times in the tidal cycle. This was done for the time-series at each model grid point closest to the UKNTGN gauge sites. In brief, as it is described in detail above, kde pdfs were calculated for the modelled high tidal level at the time of extreme skew surge, modelled tidal phase at the time of extreme non-tidal residuals, and modelled tidal level at the time of the extreme non-tidal residuals. As the modelled time-series only covered a period of 2 years, we chose to lower the threshold that defines an 'extreme' event for this aspect of the analysis to the 95th percentile to increase the sample size.

3. Results

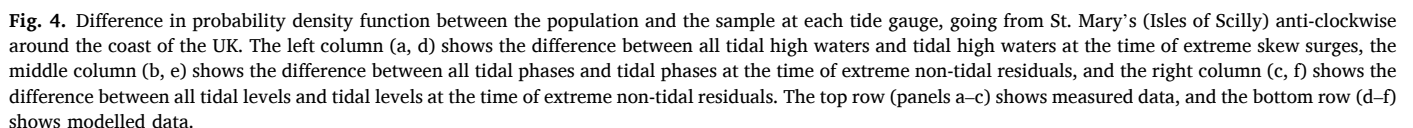
3.1. Time-series data analysis

The first objective is to test the sensitivity of tide-surge interactions to varying thresholds and declustering window lengths. To do this, we calculate pdfs for our parameters and overlay them to show the differences in the distributions' magnitude and shape that represents tide-surge interaction. We do this for each site (Fig. S1–S6, supplementary materials), but for illustration here, we use the same sites as the UKCP18 report section on projected future return level curves (Met Office, 2018), namely Avonmouth, Lerwick, Sheerness and Newlyn. Fig. 3 shows the results for these example sites, with the thresholds of the 95th, 97th, and 99th percentile, and storm windows of 32 h, 60 h, and 84 h for the tidal level and phase analysis. Overall, the differences in interaction with a changing threshold and storm window are relatively small but with larger differences in some parameters/sites. For example, the modelled pdfs at Sheerness for the distribution of tidal phase at the time of



The second objective is to determine the levels of tide-surge

interaction seen around the UK in the observational record and compare this to the levels seen in a near 500-year model run. We first do this by calculating the pdfs of the samples (1) tidal high waters at time of extreme skew surges; (2) tidal phases at time of extreme non-tidal residuals; and (3) tidal levels at the time of extreme non-tidal residuals); and the pdfs of the populations (all tidal high waters; all tidal phases; and all tidal levels) and plot the difference in magnitude across the pdf



evaluation points. Fig. 4 shows the normalised results for measured data (top row, panels a–c) and modelled data (bottom row, panels d–f), for all parameters: the difference between all predicted tidal high waters and predicted tidal high waters at the time of extreme skew surges (left column, panels a and d); the difference between all tidal phases and tidal phases at the time of extreme non-tidal residuals (middle column, panels b and e); and the difference between all tidal levels and tidal levels at the time of extreme non-tidal residuals (right column, panels c and f). Positive differences (red colours) show where the sample has a higher pdf value than the population, whereas negative differences (blue colours) show where the sample has a lower pdf value than the population. Generally, Fig. 4 shows that the measured data tends to have larger differences between the population and sample distributions than the modelled data. The lowest magnitude of interaction is seen for skew surge at the time of tidal high waters against all tidal high waters and the highest level of interaction is seen for tidal phase at the time of extreme non-tidal residuals against all non-tidal residual.

For measured skew surge shown in Fig. 4a, the Bristol Channel has the greatest level of interaction where there is a slight tendency for extreme skew surges to occur at lower magnitude tidal high waters, particularly further into the region, from Hinkley Point up and around to Newport, with Ilfracombe, Mumbles and Milford Haven not seeing any real difference in tidal high water level at the time of extreme skew surges. For the rest of the UK coast the level of interaction is of a smaller magnitude, with no dominant recurring pattern. For example, in the North Atlantic there is a slight tendency for extreme skew surges not to occur at the lower magnitude tidal high waters, and in the North Sea from Lerwick to Leith a similar pattern is seen, but then from Felixstowe to Sheerness this pattern reverses. In the other regions there is no clear spatial coherence between sites. Modelled skew surges shown in Fig. 4d see a lower level of interaction, with much of the pdf evaluation points for the whole coastline seeing values of between -0.01 and 0.1 . In the only area where a slightly stronger pattern emerges, the North Sea, extreme skew surges show a slight tendency to not occur at higher magnitude tidal high waters, instead there is a slight tendency for the extreme skew surges to occur at average, or just below average, tidal high waters. This signal is clearest in the northern North Sea, in direct contrast to the measured data.

The difference in measured tidal phase at the time of extreme non-tidal residuals and all tidal phases in Fig. 4b shows the largest levels of interaction of any of the parameters for both the measured and modelled data. There is a clear signal seen across the UK coastline that the most extreme non-tidal residuals tend not to occur at the time of, or just after, the time of tidal high water. Instead, they tend to occur relatively more frequently around 3.5 h before, or to a lesser extent, 4 h after, tidal high water. The strongest levels of interaction are seen in the Bristol Channel and in the North Sea. Dover and Newhaven in the English Channel see higher levels of interaction closer to tidal high water, showing that extreme non-tidal residuals at those tide gauge sites occur (relatively) more frequently around 1 h before tidal high water. Also, the English Channel has the only sites where the highest levels of interaction are seen for extreme non-tidal residuals after tidal high water, with Portsmouth and Weymouth having their largest levels of interaction occurring around 4–5 h after tidal high water. In the modelled results in Fig. 4e, there is a lower magnitude of interaction seen when compared to the measured tidal phases, and a slightly different overall pattern seen. Typically, most tide gauge locations still see higher levels of extreme non-tidal residuals occurring before high water, but unlike the measured results, there are not any strong examples of this interaction also occurring after high water. The largest level of interaction for any modelled data across all the parameter pairs is seen in the Bristol Channel, at Portbury, Avonmouth and Newport. These tide gauge locations see high levels of interaction from around 2 h before high water to just after high water. The other region that sees a high level of interaction is the North Sea. The modelled results mirror somewhat the measured results for the region, with extreme non-tidal residuals

tending to occur around 1–3.5 h before high water and tending not to occur from the time of high water to around 2.5 h after.

The difference in tidal level at the time of extreme non-tidal residuals and all tidal levels is shown in Fig. 4c (measured) and 4f (modelled). The measured data show a pattern whereby extreme non-tidal residuals tend to occur at tidal levels lower than the average tidal level at that site. This then transitions to no difference in likelihood as the tidal level increases to around the average, and then an increased likelihood at tidal levels above the average. However, the magnitude of the tidal levels and the resulting ‘midpoint’ between the different types of interaction, alters between regions and even neighbouring tide gauges. For example, for the Irish Sea, this ‘midpoint’ is around the average tidal level, whereas in the North Sea, it is typically of a slightly greater magnitude than the average. The Bristol Channel tide gauges of Portbury, Avonmouth and Newport see the largest interaction, with some of this interaction also occurring at the lowest tidal levels. Dover and Newhaven, in the English Channel, see the greatest levels of interaction at higher tidal levels, where, unlike the other tide gauges, there is no significant tendency for non-tidal residual extremes to occur at times when the tidal level is at or below average. Like all the parameter pairs, lower levels of interaction are seen in the modelled results. The modelled results largely match the measured results, just at a lower magnitude of interaction, except in the Bristol Channel. The tide gauge locations of Portbury, Avonmouth and Newport see the opposite signal of interaction than what would be expected from the other modelled gauges and the measured results, where it has a strong negative interaction at low tidal levels. This means that there is a strong tendency for extreme non-tidal residuals to not occur at the lower tidal levels at these gauge locations in the model.

To further determine and quantify the levels of tide-surge interaction seen around the UK in the observational record and compare this to the modelled data, we apply the Chi-squared test (χ^2) and then Cramer's V (ϕ_c) to the χ^2 results for our parameter pairs. We present the ϕ_c results spatially in Fig. 5. Measured results are shown in the top row (panels a–c) and modelled results are shown the bottom row (panels d–f). Each column represents a parameter pair (left to right): (1) tidal high waters at the time of extreme skew surges against all tidal high waters; (2) tidal phases at the time of extreme non-tidal residuals against all tidal phases; and (3) tidal levels at the time of extreme non-tidal residuals against all tidal levels. Fig. 5 shows that the ϕ_c results for tidal high waters and extreme skew surges (panels a, d) are of a far smaller magnitude than of tidal levels (panels b, e) and phases (panels c, f) at the time of extreme non-tidal residuals. There are no tide gauge sites, for measured or modelled data, where the deviation in distribution between the measured tidal high waters at the time of extreme skew surges and the expected tidal high waters is greater than $0.4 \phi_c$. The modelled data (panel d) only has three tide gauge sites where the ϕ_c values are above 0.1 , namely Wick, Aberdeen, Leith and Moray Firth. The measured data (panel a) has far more sites with ϕ_c values above 0.1 , but still none above 0.4 . Conversely, most of these sites are in the English Channel, the Bristol Channel, and the East of England. The four tide gauges that have ϕ_c values above 0.1 in the North of England are Millport, Tobermory, Stornoway and Moray Firth.

As expected from the results presented above and shown in Fig. 4, the largest ϕ_c values are seen around the UK for the tidal phases at the time of extreme non-tidal residuals. Like with the skew surge ϕ_c results, the measured results shown in Fig. 5b around the UK are typically greater than their modelled counterparts (5e). For the measured tidal phase analysis, most tide gauges see ϕ_c values of ≥ 0.3 , which indicates a moderate deviation in distribution between tidal phases at the time of extreme non-tidal residuals and expected tidal phases for most of the UK. The tide gauge sites with the largest values are Liverpool, Newport, Portbury, Jersey, Dover, Felixstowe and Cromer, who all see ϕ_c values of ≥ 0.5 . Newport, Portbury, Felixstowe and Cromer all see values ≥ 0.6 , which indicates a strong non-linear interaction for tidal phase at these sites.

There is a level of spatial coherence, with some regions seeing similar

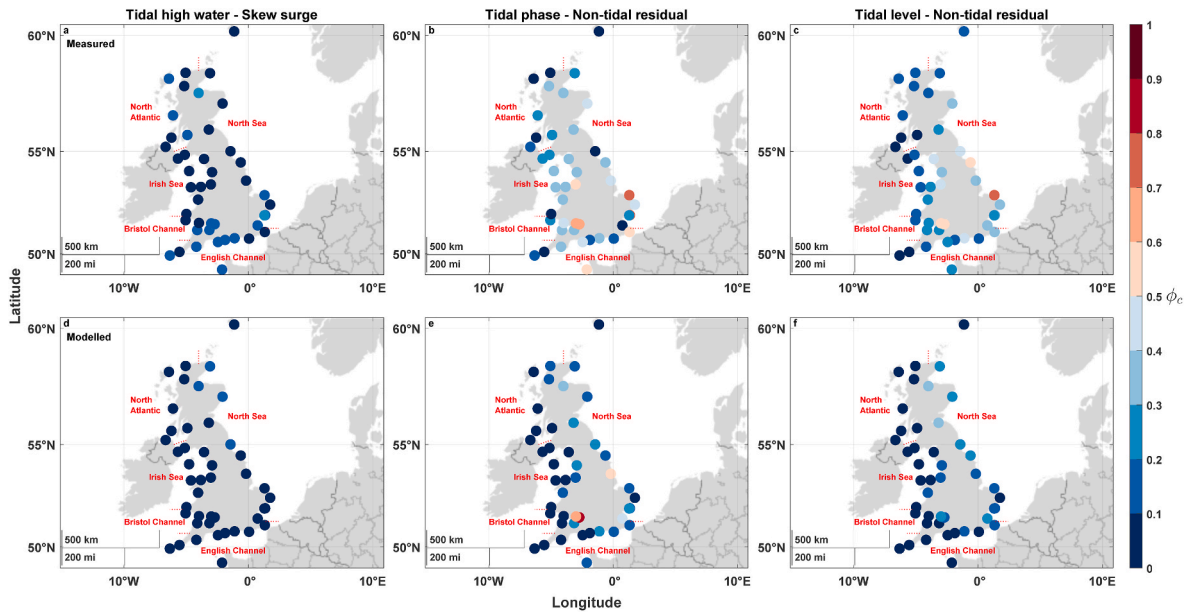


Fig. 5. Cramer's V values (ϕ_c) for the population versus the sample at each tide gauge. The left column (a, d) shows ϕ_c for all tidal high waters against tidal high waters at the time of extreme skew surges, the middle column (b, e) shows ϕ_c for all tidal phases against tidal phases at the time of extreme non-tidal residuals, and the right column (c, f) shows ϕ_c for all tidal levels against tidal levels at the time of extreme non-tidal residuals. The top row (a–c) shows measured data, and the bottom row (d–f) shows modelled data.

results. However, there are also large differences between some sites within a region. For example, Dover and Newhaven in the English Channel. The modelled tidal phase analysis shows a reduced magnitude of ϕ_c values for most tide gauges. This is particularly evident on the West coast of the UK, where most sites have ϕ_c values that are less than 0.1. There is a greater level of spatial coherence around the coastline of the UK than in the measured results. From the sites mentioned above with large ϕ_c values for the measured data, only Newport and Portbury retain a large ϕ_c value in the modelled results. Felixstowe, for instance, sees its ϕ_c value drop by ≥ 0.5 . On the other hand, Portbury has the largest ϕ_c value (≥ 0.8) for any parameter pair across both the measured and modelled data, showing the most significant deviation between the expected tidal phases and the measured tidal phases at the time of extreme non-tidal residuals.

The ϕ_c results for predicted tidal levels at the time of extreme non-tidal residuals against expected predicted tidal levels are shown in Fig. 5c for measured data and Fig. 5f for modelled data. Like all parameter pairs, the modelled results show less interaction than the measured data and both show a good level of spatial coherence. No

modelled ϕ_c results for tidal levels are greater than 0.4, with the North Sea seeing the most spatial coherence and the highest ϕ_c values, with Leith and Moray Firth having the largest ϕ_c values (≥ 0.3) in the UK. In the measured results, the North Sea still has some of the highest ϕ_c values seen, but these are instead seen in the English North Sea, rather than the Scottish coast. Cromer has the highest value (≥ 0.7 ϕ_c) of anywhere in the UK, showing a strong deviation of the distributions; with Whitby, Newport and Portbury also having large values (0.5 ϕ_c), showing a moderate deviation of the distribution of tidal levels at the time of extreme non-tidal residuals and the expected tidal levels.

3.2. Hydrodynamic modelling

The third objective is to evaluate the difference in tide-surge interaction and event magnitude with a shift in storm arrival time. To assess this, we ran the CS3 model for the years 2013 and 2014 with an artificially time-adjusted meteorological forcing and extracted the modelled time-series at the grid nodes closest to the tide gauge sites in the UKNTGN. In the same manner as the time-series analysis, the difference

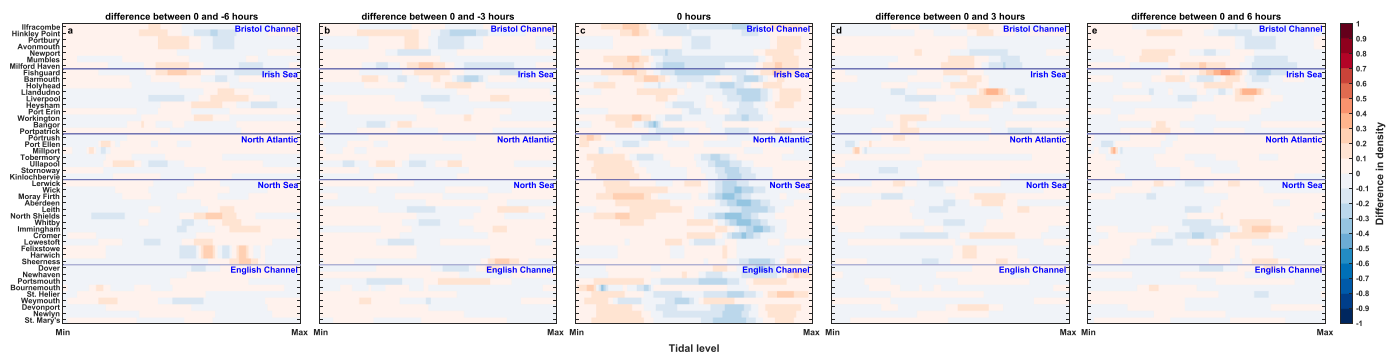


Fig. 6. Difference in probability density function between all tidal high waters and tidal high waters at the time of extreme skew surges at each tide gauge for the 2013/14 model run and subsequent time shifted runs, going from St. Mary's (Isles of Scilly) anti-clockwise around the coast of the UK. The middle panel (c) shows the results with the unadjusted forcing, whereas the other panels show the difference between the runs with the time adjusted forcing and the unadjusted run: (a) shows the difference between the -6 h time shifted run and the unadjusted run, (b) the difference between the -3 h time shifted run and the unadjusted run, (d) the difference between the $+3$ h time shifted run and the unadjusted run, and (e) the difference between the $+6$ h time shifted run and the unadjusted run.

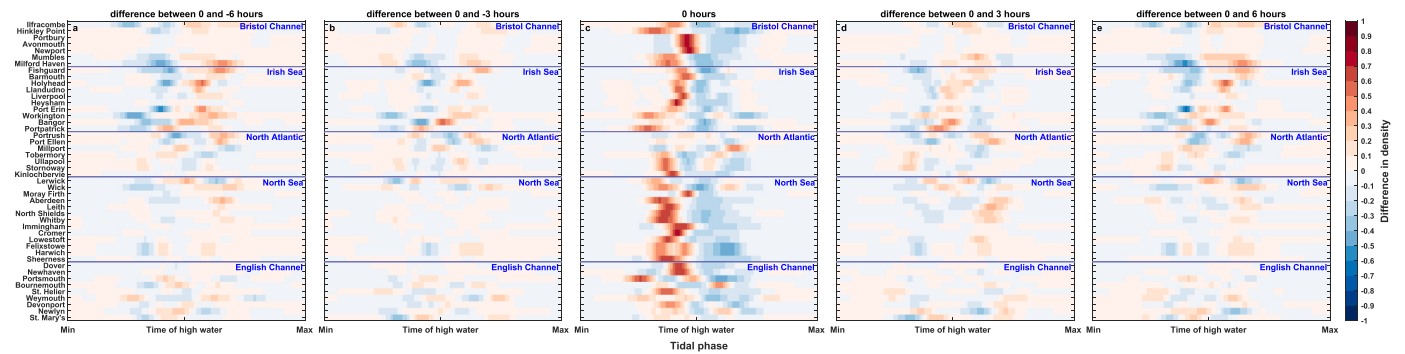


Fig. 7. Difference in probability density function between all tidal phases and tidal phases at the time of extreme non-tidal residuals at each tide gauge for the 2013/14 model run and subsequent time shifted runs, going from St. Mary's (Isles of Scilly) anti-clockwise around the coast of the UK. The middle panel (c) shows the results with the unadjusted forcing, whereas the other panels show the difference between the runs with the time adjusted forcing and the unadjusted run: (a) shows the difference between the -6 h time shifted run and the unadjusted run, (b) the difference between the -3 h time shifted run and the unadjusted run, (d) the difference between the $+3$ h time shifted run and the unadjusted run, and (e) the difference between the $+6$ h time shifted run and the unadjusted run.

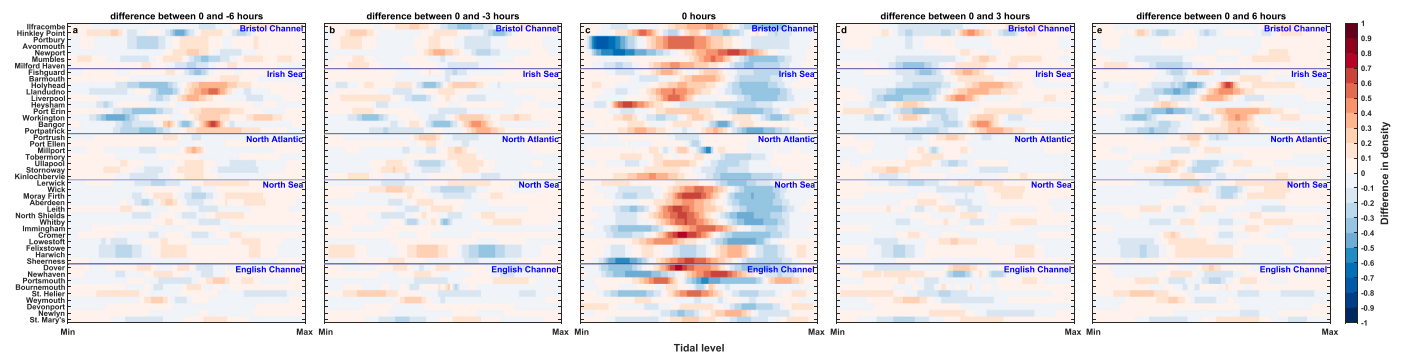


Fig. 8. Difference in probability density function between all tidal levels and tidal levels at the time of extreme non-tidal residuals at each tide gauge for the 2013/14 model run and subsequent time shifted runs, going from St. Mary's (Isles of Scilly) anti-clockwise around the coast of the UK. The middle panel (c) shows the results with the unadjusted forcing, whereas the other panels show the difference between the runs with the time adjusted forcing and the unadjusted run: (a) shows the difference between the -6 h time shifted run and the unadjusted run, (b) the difference between the -3 h time shifted run and the unadjusted run, (d) the difference between the $+3$ h time shifted run and the unadjusted run, and (e) the difference between the $+6$ h time shifted run and the unadjusted run.

between sample and population pdfs for our parameter pairs from this new data source is shown in Figs. 6–8, for the three selected parameter pairs analysed in objective 1. Each figure shows a parameter pair with the result for the unadjusted time-series (0 h) shown in panel c and the difference between the unadjusted time-series and the adjusted time-series shown in the surrounding panels. Panel a shows the difference between 0 h and -6 h, panel b the difference between 0 h and -3 h, panel d the difference between 0 h and $+3$ h, and panel e the difference between 0 h and $+6$ h. This enables the interaction for this 2013/14 period to be seen from the 0 h result and discern how this interaction changes with an artificially time-adjusted forcing.

Fig. 6 shows the results for high waters at the time of extreme skew surges against all high waters. Overall, a similarly low level of interaction is seen for this modelled subset of data (no time adjustment, 6c) as for the measured results for skew surge (Fig. 4a), but with a different pattern. The 2013/14 modelled results in Fig. 6 show more spatial coherence, with some clearer regional signals. The English Channel, Bristol Channel, and Irish Sea show a general trend of extreme skew surges tending to occur relatively less frequently at high water levels that are roughly between the ~ 25 th and ~ 75 th percentiles of all high waters, with extreme skew surges occurring relatively more frequently outside of this middle section of data (i.e., <25 th percentile and >75 th percentile). The key difference for the North Atlantic and North Sea is that negative values (indicating extreme skew surges occurring relatively less frequently) are not typically seen around the average tidal high water level. Instead, all occur at higher levels; and, apart from Sheerness, there are no significant positive values (indicating extreme

skew surges occurring relatively more frequently) that occur at tidal high water levels that are greater than the average of all tidal high water levels for this period. As the forcing is moved backwards (panels a–b) and forwards (panels d–e) in time, this change does not greatly affect the relative tendencies of when extreme skew surges occurred. For most tide gauges across all the time shifted results, the differences seen were small in magnitude (≤ 0.1) along the sample points of tidal high water level. The largest differences seen are for Llandudno and Fishguard in the Irish Sea. As the forcing is moved forwards in time, Llandudno sees a significant positive change at higher tidal levels where at 0 h there was a tendency for relatively less extreme skew surges to occur. There is also a significant positive change at Fishguard for tidal high water levels slightly above the average, that at 0 h saw a tendency for relatively less extreme skew surges to occur. Interestingly, this change is only seen at the $+6$ h time shift, and not at $+3$ h.

The 2013/14 model run results for tidal phase are shown in Fig. 7. For the unaltered forcing results (7c), the strength of interaction seen is also similar to the measured time-series (Fig. 4b). However, the pattern seen is more akin to the results from the 500-year model run (Fig. 4e), with few examples of higher levels of extreme non-tidal residuals occurring after high water, as most positive interactions occur just before tidal high water, and most negative interaction occurs just after tidal high water. These interactions are nearer the time of high water than in the modelled 500-year run, with a smaller spread. As the meteorological forcing is moved backwards and forwards in time, larger differences between the time shifted results and the 0 h unaltered results are seen than for skew surges (Fig. 6). Typically, the time shifted results

show that changes to the interaction seen at 0 h are in the opposite direction to the initial interaction. I.e., a positive value at 0 h, indicating a higher relative tendency for extreme non-tidal residuals to occur at that tidal phase, would typically get smaller after time adjustment, indicating a reduction in that tendency. The pattern, though, changes by region (Fig. 7). For example, in the +3 h time adjustment (panel d), most positive changes in the Irish Sea are seen at the time of high water, whereas in the North Sea, most of the positive changes are seen a couple of hours after tidal high water. The -3 h (panel b) and +3 h time adjustments see similar results, with the -3 h results seeing some stronger negative changes and the +3 h results having more tide gauges seeing changes greater than ± 0.1 along the sample points. Interestingly, for the -6 h (panel a) and +6 h (panel e) adjustments, there is very little difference between the results.

Fig. 8 shows the difference in distribution of tidal levels at the time of extreme non-tidal residuals and all tidal levels for the 2013/14 modelled data. Without any time shifting of the forcing data (Fig. 8c), again, the level of interaction seen is similar to the measured results in Fig. 4c and greater than the 500-year model results in Fig. 4f. The pattern is also similar to the measured data, but with some key differences. Overall, gauges tend to show a positive level of interaction (indicating a greater relative tendency of extreme non-tidal residual occurrence) nearer the average tidal level when compared to the measured results. The most obvious difference is the considerable change in signal in the Bristol Channel. Hinkley Point has a similar signal to the modelled data, but all other tide gauges in the Bristol Channel see positive signals at higher tidal levels than in the measured data, particularly at Ilfracombe, Newport and Mumbles where the strongest level of positive interaction seen is at tidal levels above the average. The strongest negative interactions (Fig. 8c) are seen at Portbury, Avonmouth and Newport, where the strongest positive interactions occur at tidal levels close to the minimum for the 2013/14 model run, in contrast to the measured data (Fig. 4c). This indicates a strong tendency for extreme non-tidal residuals to occur relatively less frequently at the lowest tidal levels in 2013/14. There are also stronger negative interactions seen at lower tidal levels in the North Sea and English Channel when compared to the measured time-series results. When the forcing is time shifted (panels a–b, d–e), like the results for tidal phase, the greatest changes in interaction are seen in the Irish Sea. When the time shifting is at its maximum (-6 and +6 h, panels a and e, respectively), model grid nodes at the locations of the tide gauges in the Irish Sea show a comparable pattern of change with most sites seeing negative differences below their respective average tidal level and positive differences above. The difference for the +3 h time shift (Fig. 8d) also sees a comparable pattern in the Irish Sea, whereas for the -3 h time shift this pattern is less evident. In the other regions, there is not a consistent pattern across the time shifted results and differences are typically of a reduced magnitude.

4. Discussion

In this paper, we have assessed non-linear tide-surge interactions around the UK coast using both measured data and a near 500-year model dataset through the lens of skew surge against tidal high water, non-tidal residual against tidal phase, and non-tidal residual against tidal level; the three main approaches used to assess tide-surge interaction, which to our knowledge, have not been compared in detail before now. We show that there are substantial tide-surge interactions around the UK coastline between the non-tidal residual and the astronomical tide. As Horsburgh and Wilson (2007) and Haigh et al. (2010) showed, tide-surge interactions can be different on the ebb and flood phases of the tide, so it is important to not just consider tidal level but also the tidal phase. We find that the largest levels of interaction for any of the parameters are for tidal phase at the time of extreme non-tidal residuals. At almost all tide gauges, measured extreme non-tidal residuals tend to occur relatively more frequently between 1 and 5 h before tidal high water, relatively less frequently from 1 h before tidal

high water to 2.5 h after, and relatively more frequently again, but to a lesser magnitude and at fewer tide gauges, between 3 and 5.5 h after tidal high water. This is also seen in the interaction between tidal level at the time of extreme non-tidal residual, where almost all tide gauges see increased tendencies for extreme non-tidal residuals to occur below the average tidal level, and decreased tendencies for tidal levels above the average. The significance of these interactions varies in space, with the Bristol Channel tide gauges of Newport and Portbury being the standout sites that saw high levels of interaction across all parameters and tests, likely due to the Bristol Channel having the largest tidal range in the UK. The tendency for extreme non-tidal residuals to occur at lower tidal levels and on the flood tide is likely a result of a phase shift of the tidal signal, rather than a true meteorological influence. It does confirm, as Williams et al. (2016) stressed, that the analysis of non-tidal residuals is problematic since there is not always a genuine meteorological contribution to large residuals. Our results also concur with those of Williams et al. (2016) in that the interaction between high tide and extreme skew surges is much less pronounced compared to the non-tidal residual. We would therefore recommend that any sea level analysis for UKNTGN sites should focus on skew surges and not the non-tidal residual, and that the assumption of independence between high tides and skew surges used for the estimation of extreme sea level probabilities in the latest 2018 UK coastal flood boundary conditions report (Environment Agency, 2018) is appropriate.

The foundation of analysis from this study was built from Horsburgh and Wilson (2007), Haigh et al. (2010) and Williams et al. (2016). Our analysis tended to produce similar results to their studies and agrees with their conclusions, even with our different data temporal ranges and methodological adjustments. The use of normalised probability distributions in Horsburgh and Wilson (2007) and Williams et al. (2016) to show the nature of interactions do not see significant differences to our results, despite our data having an increased number of years, and therefore extreme events. Our results for the tidal phase and extreme non-tidal residuals Cramer's V analysis at English Channel tide gauge sites, although not directly comparable, also align with the magnitude of Haigh et al.'s (2010) Chi-squared results. Although no significant change in value magnitude is seen here for the small number of overlapping sites, we propose that using Cramer's V for this approach is beneficial as it negates the influence of sample size and produces results that are easier to interpret than Chi-squared.

Comparing the sensitivities of the chosen example sites to a changing threshold and storm window, a similar interpretation is drawn to the results from all the UKNTGN sites, in that, although there are some differences seen for certain parameters when the threshold and storm window changes. These differences tend to be small in magnitude and not greatly affect the overall distribution shape. Some sites see more difference than others however, for example in Fig. 3, measured high waters at the time of extreme skew surges at Avonmouth, or modelled tidal phases at the time of extreme non-tidal residuals at Sheerness. Nonetheless, overall, it is proposed that an exhaustive selection process of threshold and declustering window for the wider analysis of tide-surge interaction around the UK is not mandatory, as the general difference in distribution magnitude and shape is not of great significance. For the intricate analysis of individual sites and individual parameters, a more detailed approach may prove beneficial, such as for specific high risk coastal assets or defences such as storm surge barriers and nuclear power stations.

Although there is a level of spatial coherence between sites in our analysis for the signal of interaction, there are no clear regional patterns for the strength of interaction that was measured using Chi-squared and Cramer's V. As storm surges in the UK typically affect large parts of the coastline and multiple tide gauge sites, it is likely that neighbouring sites often see extreme non-tidal residuals occur at similar stages of the tide and therefore experience some commonality to the tide-surge interaction. However, as the spatial coherence is not seen in the strength of interaction, it is likely that local effects, such as bathymetry, could be

driving those differences. For example, there are occasions where nearby sites experience different levels of interaction — the measured ϕ_c results for tidal phase saw a significant difference between Harwich and Felixstowe, despite the tide gauges being less than 4 km away from each other. Local effects would best explain this, as well as the influence of storm direction in relation to the orientation of the coast. Similar differences in Chi-squared values between sites were seen in the English Channel by Haigh et al. (2010), but also in other parts of the world such as the coast of China (Feng et al., 2019) and the east coast of India (Antony and Unnikrishnan, 2013) as the strength of non-linear tide-surge interactions tends to be site specific.

The tide gauges of Harwich and Felixstowe also have different temporal ranges, and more detailed up-to-date analysis into the changing of non-linear tide-surge interaction signals through time, or in different periods, would be of interest. This would be especially relevant in relation to temporally clustered periods (e.g., Jenkins et al., 2023), as although we show that there is not much variation in interaction with a changing magnitude of event, other storm characteristics, such as repeat time, would be of interest to evaluate in the context of non-linear tide-surge interaction.

Our use of observational records means that there is a change of temporal frequency pre- and post-1993 from hourly to every 15-min. The coarser frequency may mask some interactions, but we expect that this effect will be minimal in context of the duration of UK surges (Haigh et al., 2016; Jenkins et al., 2023) and tides. The difference in calculation of tides for the measured and modelled analysis might have produced slightly differing tidal levels. However, it is also unlikely that such minor variation would have had any impact on the levels of interaction seen in the timeseries.

In this study, the near 500-year modelled results consistently showed a lower level of tide-surge interaction than the measured results. Although some of the overall patterns seen in the measured results were captured in the near 500-year model, many were not adequately captured, and nearly all would be of a lower level of interaction. A more comparable level of interaction was seen in the 2013/14 model run, the stormiest winter season on record in the UK, and, as discussed above, further investigation into the difference in interaction depending on the time period analysed would be of interest. However, models do tend to struggle in accurately representing extremes (Sillmann et al., 2017), for example, Jenkins et al. (2023) highlighted key differences between measured extreme surges in the UK and a modelled hindcast, and in Jenkins et al., 2024, where the authors used the same near 500-year modelled dataset used in this paper, the model was shown to underperform slightly in representing the measured levels of temporal clustering of extreme surges. It is probable that the coarse spatial resolution of such large-scale hydrodynamic models, combined with the complex bathymetry of the UK coastline, could cause some of the underestimation in non-linear tide-surge interaction seen. It has been noted that shelf models such as CS3 cannot fully represent areas such as the Bristol Channel that have large tidal ranges and strong interactions (Flather, 2000). Nonetheless, models are the only way of gaining continuous, gap-free coverage around the UK coastline and play a major role in UK surge forecasting and emergency preparedness planning. As tide-surge interaction is critical to the realisation of extreme sea levels which lead to flooding at the coast, it is crucial that the representation of tide-surge interaction continues to improve in coastal surge models.

Our time shifted analysis shows that, while there were differences with the levels of tide-surge interaction between the time shifts, these differences were not seen on a UK-wide scale and did not have clear coherence as the forcing time changed. Overall, for most sites, the magnitude of change was also not that large (typically around ± 0.2), suggesting that while the varying arrival time of a storm can affect the timing (tidal phase) and tidal level at the time of the maximum surge, it is more likely that the maximum surge will occur at the same tidal times/levels of the other maximum surges in the time series. Changes of ± 6 h in storm arrival time had little effect on the tide-surge interaction

for skew surge, as one could predict. The largest differences seen were actually between the 2013/14 subset of data and the other full time series results. To enhance this study, we would recommend that the model runs with the meteorological time shifts be applied to a longer period of 10–20 years, so that the extra data could more accurately represent the impact of change in storm arrival time on tide-surge interaction. With extended time series, extreme sea level probabilities for the time adjusted time series could be calculated around the coast of the UK, showing if there would be a change in return levels, and the impact of using non-tidal residual against skew surge in such estimations of water level return periods could be assessed more fully.

A limitation of our method was the lack of physical analysis to link specific mechanisms to the interaction seen. Although the mechanisms of non-linear tide-surge interaction in the UK are well known (e.g., Proudman, 1957, 1955; Rossiter, 1961; Prandle and Wolf, 1978a, 1978b; Horsburgh and Wilson, 2007), as we focused on purely timeseries data and the reporting of interaction, although it is highly likely that the previously reported mechanisms are driving the interaction seen here, we cannot confirm this. Future research that explores the physical mechanisms of the interaction seen here in relation to the observed propagation of surge events in the UK (Haigh et al., 2016; Camus et al., 2024) would be of interest.

5. Conclusions

In this study we assessed non-linear tide surge interactions around the UK coast. We used measured and modelled sea level time-series data analysis combined with a complementary hydrodynamic modelling exercise, in which we artificially adjusted meteorological forcing backward and forward in time to coincide with different stages of the tide, to systematically assess the prevalence, characteristics, and importance of non-linear tide-surge interactions around the United Kingdom. For the first time, we compared and contrasted the different methods that have been used to assess non-linear tide-surge interactions in past studies and importantly show how the results can differ depending on which parameter is used in the analysis (i.e., skew surge; tidal level; or tidal phase). Results from both the data analysis and modelling exercise show there are considerable non-linear interactions between the non-tidal residual (defined as being total water level minus astronomical tide) and the astronomical tide, both in terms of tidal level and phase. Extreme non-tidal residuals in the UK tend to occur relatively more frequently primarily before (strongest signal at -3.5 h), and to a lesser extent, after (strongest signal at $+4$ h), tidal high water, and at tidal levels at, or below, the average for that site. In contrast, although there is some level of non-linear interaction between skew surge and tidal high waters, the extent of this interaction is negligible when compared to the other parameters and one can conclude that the two are virtually independent. Tide-surge interactions were under-represented in the modelled data, which may have implications for the forecasting of coastal extreme sea levels. Change in storm arrival time can affect the level of non-linear tide-surge interaction, even on a regional scale, but the results suggest that greater differences in UK-wide signal are seen when analysing different periods. As the combination of tide and surge constitute the main component of extreme sea levels, which drive coastal flooding, it is critical that non-linear tide-surge interaction is fully understood. Accurately representing such interaction is a key element of robustly calculating extreme sea level probabilities that are used to monitor the coast and warn against coastal flooding.

CRedit authorship contribution statement

Luke J. Jenkins: Writing – review & editing, Writing – original draft, Visualization, Software, Methodology, Investigation, Formal analysis, Data curation, Conceptualization. **Ivan D. Haigh:** Writing – review & editing, Software, Methodology, Investigation. **Dafni E. Sifnoti:** Writing – review & editing, Software, Methodology, Investigation,

Conceptualization. **Jose Alejandro Pinto Rascon:** Writing – review & editing, Methodology, Investigation, Conceptualization. **Addina Inayatillah:** Software, Methodology, Formal analysis, Data curation. **Hachem Kassem:** Writing – review & editing, Funding acquisition, Conceptualization.

Funding sources

Luke J. Jenkins is funded through the Natural England Research Council (NERC) INSPIRE Doctoral Training Program (grant number NE/S007210/1) and is co-sponsored by the JBA Trust. Part of the work was funded by EDF Energy R&D Centre Limited (Project UoS-516711113: Tide-Surge Interaction at UK Nuclear Sites, PI: Hachem Kassem).

Declaration of competing interest

The authors declare the following financial interests/personal relationships which may be considered as potential competing interests: Luke J. Jenkins reports financial support was provided by UK Research and Innovation Natural Environment Research Council. Luke J. Jenkins reports financial support was provided by EDF Energy Research and Development. Hachem Kassem reports financial support was provided by EDF Energy Research and Development. Ivan D. Haigh reports financial support was provided by EDF Energy Research and Development. Addina Inayatillah reports financial support was provided by EDF Energy Research and Development. If there are other authors, they declare that they have no known competing financial interests or personal relationships that could have appeared to influence the work reported in this paper.

Acknowledgements

We acknowledge the use of the IRIDIS High Performance Computing Facility, and associated support services at the University of Southampton.

Appendix A. Supplementary data

Supplementary data to this article can be found online at <https://doi.org/10.1016/j.ecss.2025.109323>.

Data availability

The measured still sea level records from the United Kingdom National Tide Gauge Network are available from the British Oceanographic Data Centre: https://www.bodc.ac.uk/data/hosted_data_systems/sea_level/uk_tide_gauge_network/. The near 500-year model timeseries of sea levels and tides is available on request from the primary author of Howard and Williams (2021) DOI: <https://doi.org/10.5194/nhess-21-3693-2021>. The ERA5 *u* and *v*-components of wind velocity (10m) and mean sea level pressure can be downloaded from <https://www.ecmwf.int/en/forecasts/datasets/browse-reanalysis-datasets> DOI: <https://doi.org/10.1002/qj.3803>.

References

Antony, C., Unnikrishnan, A.S., 2013. Observed characteristics of tide-surge interaction along the east coast of India and the head of Bay of Bengal. *Estuar. Coast Shelf Sci.* 131, 6–11. <https://doi.org/10.1016/j.ecss.2013.08.004>.

Arns, A., Wahl, T., Wolff, C., Vafeidis, A.T., Haigh, I.D., Woodworth, P., Niehüser, S., Jensen, J., 2020. Non-linear interaction modulates global extreme sea levels, coastal flood exposure, and impacts. *Nat. Commun.* 11, 1918. <https://doi.org/10.1038/s41467-020-15752-5>.

Batstone, C., Lawless, M., Tawn, J., Horsburgh, K., Blackman, D., McMillan, A., Worth, D., Laeger, S., Hunt, T., 2013. A UK best-practice approach for extreme sea-level analysis along complex topographic coastlines. *Ocean. Eng.* 71, 28–39. <https://doi.org/10.1016/j.oceaneng.2013.02.003>. Sea Level Rise and Impacts on Engineering Practice.

Botev, Z.I., Grotowski, J.F., Kroese, D.P., 2010. Kernel density estimation via diffusion. *Ann. Stat.* 38, 2916–2957. <https://doi.org/10.1214/10-AOS799>.

Cabinet Office, 2020. *National Risk Register*.

Camus, P., Haigh, I.D., Quinn, N., Wahl, T., Benson, T., Gouldby, B., Nasr, A.A., Rashid, M.M., Enríquez, A.R., Darby, S.E., Nicholls, R.J., Nadal-Caraballo, N.C., 2024. Tracking the spatial footprints of extreme storm surges around the coastline of the UK and Ireland. *Weather Clim. Extrem.* 44, 100662. <https://doi.org/10.1016/j.wace.2024.100662>.

Codiga, D., 2022. *UTide Unified Tidal Analysis and Prediction Functions*.

de Vries, H., Breton, M., de Mulder, T., Krestenitis, Y., Ozer, J., Proctor, R., Ruddick, K., Salomon, J.C., Voorrips, A., 1995. A comparison of 2D storm surge models applied to three shallow European seas. *Environ. Software* 10, 23–42. [https://doi.org/10.1016/0266-9838\(95\)00003-4](https://doi.org/10.1016/0266-9838(95)00003-4).

Dinapoli, M.G., Simionato, C.G., Moreira, D., 2021. Nonlinear Interaction Between the Tide and the Storm Surge with the Current due to the River Flow in the Río de la Plata. *Estuaries Coasts* 44, 939–959. <https://doi.org/10.1007/s12237-020-00844-8>.

Dixon, M.J., Tawn, J.A., 1994. extreme sea-LEVELS at the UK a-class sites: site-by-site analyses. *Proudman Oceanogr. Lab. Intern. Doc.* 65.

Doodson, A.T., 1929. The monthly record. *Geogr. J.* 74, 505–511.

Environment Agency, 2018. *Coastal Flood Boundary Conditions for the UK: Update 2018. Technical Summary Report*. Environment Agency, Bristol.

Feng, J., Jiang, W., Li, D., Liu, Q., Wang, H., Liu, K., 2019. Characteristics of tide-surge interaction and its roles in the distribution of surge residuals along the coast of China. *J. Oceanogr.* 75, 225–234. <https://doi.org/10.1007/s10872-018-0495-8>.

Flather, R.A., 2000. Existing operational oceanography. *Coast. Eng.* 41, 13–40. [https://doi.org/10.1016/S0378-3839\(00\)00025-9](https://doi.org/10.1016/S0378-3839(00)00025-9).

Flather, R.A., Proctor, R., Wolf, J., 1991. Oceanographic forecast models. In: Farmer, D. G., Rycroft, M.J. (Eds.), *Computer Modelling in the Environmental Sciences*. Clarendon Press, Oxford, pp. 15–30.

Haigh, I., Nicholls, R., Wells, N., 2010. Assessing changes in extreme sea levels: application to the English Channel, 1900–2006. *Cont. Shelf Res.* 30, 1042–1055. <https://doi.org/10.1016/j.csr.2010.02.002>.

Haigh, I., Nicholls, R., Wells, N., 2009. Mean sea level trends around the English Channel over the 20th century and their wider context. *Cont. Shelf Res.* 29, 2083–2098. <https://doi.org/10.1016/j.csr.2009.07.013>.

Haigh, I.D., Nicholls, R.J., Penning-Rowsell, E.C., Sayers, P., 2022. Climate change impacts on coastal flooding relevant to the UK and Ireland. *MCCIP Sci. Rev.* 2022, 18. <https://doi.org/10.14465/2022.REU02.CFL>.

Haigh, I.D., Wadey, M.P., Wahl, T., Ozsoy, O., Nicholls, R.J., Brown, J.M., Horsburgh, K., Gouldby, B., 2016. Spatial and temporal analysis of extreme sea level and storm surge events around the coastline of the UK. *Sci. Data* 3, 160107. <https://doi.org/10.1038/sdata.2016.107>.

Haigh, I.D., Wijeratne, E.M.S., MacPherson, L.R., Pattiaratchi, C.B., Mason, M.S., Crompton, R.P., George, S., 2014. Estimating present day extreme water level exceedance probabilities around the coastline of Australia: tides, extra-tropical storm surges and mean sea level. *Clim. Dyn.* 42, 121–138. <https://doi.org/10.1007/s00382-012-1652-1>.

Hersbach, H., Bell, B., Berrisford, P., Hirahara, S., Horányi, A., Muñoz-Sabater, J., Nicolas, J., Peubey, C., Radu, R., Schepers, D., Simmons, A., Soci, C., Abdalla, S., Abellan, X., Balsamo, G., Bechtold, P., Biavati, G., Bidlot, J., Bonavita, M., De Chiara, G., Dahlgren, P., Dee, D., Diamantakis, M., Dragani, R., Flemming, J., Forbes, R., Fuentes, M., Geer, A., Haimberger, L., Healy, S., Hogan, R.J., Hólm, E., Janisková, M., Keeley, S., Laloyaux, P., Lopez, P., Lupu, C., Radnoti, G., de Rosnay, P., Rozum, I., Vamborg, F., Villaume, S., Thépaut, J.-N., 2020. The ERA5 global reanalysis. *Q. J. R. Meteorol. Soc.* 146, 1999–2049. <https://doi.org/10.1002/qj.3803>.

Horsburgh, K.J., Wilson, C., 2007. Tide-surge interaction and its role in the distribution of surge residuals in the North Sea. *J. Geophys. Res. Oceans* 112. <https://doi.org/10.1029/2006JC004033>.

Howard, T., Williams, S.D.P., 2021. Towards using state-of-the-art climate models to help constrain estimates of unprecedented UK storm surges. *Nat. Hazards Earth Syst. Sci.* 21, 3693–3712. <https://doi.org/10.5194/nhess-21-3693-2021>.

Hu, S., Liu, B., Hu, M., Yu, X., Deng, Z., Zeng, H., Zhang, M., Li, D., 2023. Quantification of the nonlinear interaction among the tide, surge and river in Pearl River Estuary. *Estuar. Coast Shelf Sci.* 290, 108415. <https://doi.org/10.1016/j.ecss.2023.108415>.

Jenkins, L.J., Haigh, I.D., Kassem, H., Pender, D., Sansom, J., Lamb, R., Howard, T., 2024. Assessing the temporal clustering of coastal storm tide hazards under natural variability in a near 500-year model run. *PREPRINT (Version 1)* available at Research Square <https://doi.org/10.21203/rs.3.rs-5439592/v1>.

Jenkins, L.J., Haigh, I.D., Camus, P., Pender, D., Sansom, J., Lamb, R., Kassem, H., 2023. The temporal clustering of storm surge, wave height, and high sea level exceedances around the UK coastline. *Nat. Hazards* 115, 1761–1797. <https://doi.org/10.1007/s11069-022-05617-z>.

Matthews, T., Murphy, C., Wilby, R.L., Harrigan, S., 2014. Stormiest winter on record for Ireland and UK. *Nat. Clim. Change* 4, 738–740. <https://doi.org/10.1038/nclimate2336>.

McRobie, A., Spencer, T., Gerritsen, H., 2005. The big flood: North Sea storm surge. *Philos. Trans. R. Soc. Math. Phys. Eng. Sci.* 363, 1263–1270. <https://doi.org/10.1098/rsta.2005.1567>.

Met Office, 2018. *UKCP18 Marine Report*.

Prandle, D., Wolf, J., 1978a. Surge-tide interaction in the southern North Sea. In: Nihoul, J.C.J. (Ed.), *Elsevier Oceanography Series, Hydrodynamics of Estuaries and Fjords*. Elsevier, pp. 161–185. [https://doi.org/10.1016/S0422-9894\(08\)71277-7](https://doi.org/10.1016/S0422-9894(08)71277-7).

Prandle, D., Wolf, J., 1978b. The interaction of surge and tide in the North Sea and river Thames. *Geophys. J. Int.* 55, 203–216. <https://doi.org/10.1111/j.1365-246X.1978.tb04758.x>.

- Priestley, M.D.K., Pinto, J.G., Dacre, H.F., Shaffrey, L.C., 2017. The role of cyclone clustering during the stormy winter of 2013/2014. *Weather* 72, 187–192. <https://doi.org/10.1002/wea.3025>.
- Proudman, J., 1957. Oscillations of tide and surge in an estuary of finite length. *J. Fluid Mech.* 2, 371–382. <https://doi.org/10.1017/S002211205700018X>.
- Proudman, J., 1955. The propagation of tide and surge in an estuary. *Proc. R. Soc. Lond. Ser. Math. Phys. Sci.* 231, 8–24.
- Pugh, D., Woodworth, P., 2014. *Sea-Level Science: Understanding Tides, Surges, Tsunamis and Mean Sea-Level Changes*. Cambridge University Press, Cambridge. <https://doi.org/10.1017/CBO9781139235778>.
- Rossiter, J.R., 1961. Interaction between tide and surge in the Thames. *Geophys. J. Int.* 6, 29–53. <https://doi.org/10.1111/j.1365-246X.1961.tb02960.x>.
- Sayers, P.B., Penning-Rowsell, E., McKenzie, A., 2015. *Climate Change Risk Assessment 2017: Projections of Future Flood Risk in the UK*. Committee on Climate Change, London.
- Sillmann, J., Thorarindottir, T., Keenlyside, N., Schaller, N., Alexander, L.V., Hegerl, G., Seneviratne, S.I., Vautard, R., Zhang, X., Zwiers, F.W., 2017. Understanding, modeling and predicting weather and climate extremes: challenges and opportunities. *Weather Clim. Extrem.* 18, 65–74. <https://doi.org/10.1016/j.wace.2017.10.003>.
- Silverman, B.W., 1986. *Density Estimation for Statistics and Data Analysis*. Chapman & Hall, London.
- Song, H., Kuang, C., Gu, J., Zou, Q., Liang, H., Sun, X., Ma, Z., 2020. Nonlinear tide-surge-wave interaction at a shallow coast with large scale sequential harbor constructions. *Estuar. Coast Shelf Sci.* 233, 106543. <https://doi.org/10.1016/j.ecss.2019.106543>.
- Wadey, M.P., Brown, J.M., Haigh, I.D., Dolphin, T., Wisse, P., 2015. Assessment and comparison of extreme sea levels and waves during the 2013/14 storm season in two UK coastal regions. *Nat. Hazards Earth Syst. Sci.* 15, 2209–2225. <https://doi.org/10.5194/nhess-15-2209-2015>.
- Williams, J., Horsburgh, K.J., Williams, J.A., Proctor, R.N.F., 2016. Tide and skew surge independence: new insights for flood risk. *Geophys. Res. Lett.* 43, 6410–6417. <https://doi.org/10.1002/2016GL069522>.
- Williams, K.D., Copsey, D., Blockley, E.W., Bodas-Salcedo, A., Calvert, D., Comer, R., Davis, P., Graham, T., Hewitt, H.T., Hill, R., Hyder, P., Ineson, S., Johns, T.C., Keen, A.B., Lee, R.W., Megann, A., Milton, S.F., Rae, J.G.L., Roberts, M.J., Scaife, A.A., Schiemann, R., Storkey, D., Thorpe, L., Watterson, I.G., Walters, D.N., West, A., Wood, R.A., Woollings, T., Xavier, P.K., 2018. The Met Office global coupled model 3.0 and 3.1 (GC3.0 and GC3.1) configurations. *J. Adv. Model. Earth Syst.* 10, 357–380. <https://doi.org/10.1002/2017MS001115>.
- Woodworth, P.L., Teferle, F.N., Bingley, R.M., Shennan, I., Williams, S.D.P., 2009. Trends in UK mean sea level revisited. *Geophys. J. Int.* 176, 19–30. <https://doi.org/10.1111/j.1365-246X.2008.03942.x>.
- Xiao, Z., Yang, Z., Wang, T., Sun, N., Wigmosta, M., Judi, D., 2021. Characterizing the non-linear interactions between tide, storm surge, and river flow in the Delaware bay estuary, United States. *Front. Mar. Sci.* 8. <https://doi.org/10.3389/fmars.2021.715557>.
- Yang, S., Sheng, J., Ohashi, K., Yang, B., Chen, S., Xing, J., 2023. Non-linear interactions between tides and storm surges during extreme weather events over the eastern Canadian shelf. *Ocean Dyn.* 73, 279–301. <https://doi.org/10.1007/s10236-023-01556-w>.
- Zhang, W.-Z., Shi, F., Hong, H.-S., Shang, S.-P., Kirby, J.T., 2010. Tide-surge interaction intensified by the Taiwan strait. *J. Geophys. Res. Oceans* 115. <https://doi.org/10.1029/2009JC005762>.